analytical chemistry

Article

Cite This: *Anal. Chem.* 2018, 90, 11439−11445

pubs.acs.org/ac

Click Chemistry Reaction-Triggered 3D DNA Walking Machine for Sensitive Electrochemical Detection of Copper Ion

Min Qing,[†,‡] Shunbi Xie,[†] Wei Cai,[†,‡] Dianyong Tang,[†] Ying Tang,[*,†] Jin Zhang,[§] and Ruo Yuan[*,‡]

[†]Chongqing Key Laboratory of Environmental Materials and Remediation Technologies (Chongqing University of Arts and Sciences), Chongqing University of Arts and Sciences, Chongqing 402160, P.R. China

[‡]Key Laboratory of Luminescent and Real-Time Analytical Chemistry (Southwest University), Ministry of Education, College of Chemistry and Chemical Engineering, Southwest University, Chongqing 400715, P.R. China

[§]Chongqing Vocational Institute of Engineering, Chongqing 402260, P.R. China

Supporting Information

ABSTRACT: Herein, for the first time, we engineered click chemistry reaction to trigger a 3D DNA walking machine for ultrasensitive electrochemical detection of copper ion (Cu^{2+}), which provided a convenient access to overcome the shortcomings of poor selectivity and limited amplification efficiency in traditional determination of Cu^{2+}. Click chemistry reaction drove azido-S2 to bind with alkynyl-S1 for the formation of a walker probe on aminated magnetic polystyrene microsphere@gold nanoparticles (PSC@Au), which opened the hairpin-locked DNAzyme. In the presence of magnesium ion (Mg^{2+}), the unlocked DNAzyme was activated to cleave the self-strand at the facing ribonucleotide site, accompanied by the release of product DNA (S3) and the walker probe. Therefore, the walker probe was able to open the adjacent hairpin-locked DNAzyme strand and then be released by DNAzyme cleavage along the PSC@Au-DNAzyme track. Eventually, the liberated single-strand S3 induced catalytic hairpin assembly (CHA) recycling, resulting in the capture of a large number of methylene blue-tagged hairpin DNA (MB-H2) on the sensor surface and significant electrochemical responses. By coupling click chemistry reaction with the dual-amplification strategy of the 3D DNA walking machine and CHA recycling, the proposed biosensor not only demonstrated high accuracy and selectivity for Cu^{2+} detection in real samples but also showed excellent performance for Cu^{2+} detection with a wide linear range of 1.0 pM to 500 nM and low detection limit of 0.33 pM. Moreover, this elaborated biosensor could be readily expanded to Mg^{2+} detection with a constant concentration of Cu^{2+}, which paves a new way to apply the 3D DNA walking machine in various ion sensings.

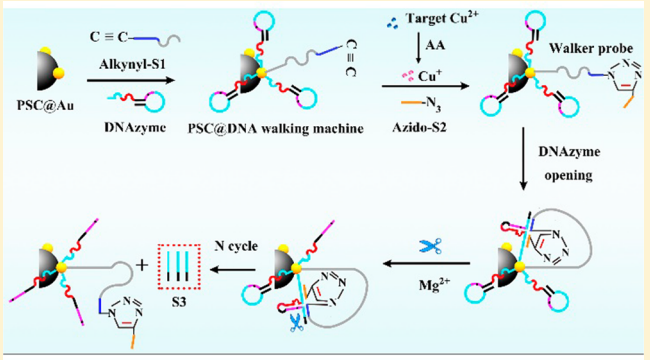

Copper ion (Cu^{2+}), one of the essential micronutrients in metabolic processes, has multiple functions for life, including electron transduction, enzyme catalysis, and oxygen transport. Abnormal Cu^{2+} levels in the body can cause adverse health effects, such as copper deficiency diseases, liver and kidney damage, and even serious neurodegenerative diseases.[1,2] It is therefore of great importance for human health to develop a simple, reliable, and ultrasensitive method to monitor and sense the Cu^{2+} levels in water. To date, a variety of strategies have been developed for Cu^{2+} detection based on small organic molecules,[3,4] nanomaterials[5−7] and biomaterials.[8−10] However, they are generally accompanied by some drawbacks including complicated organic synthesis, poor sensitivity and selectivity, and the use of toxic chemicals. Alternatively, click chemistry reaction has been used widely in sensing systems due to characteristic advantages including high selectivity, superior ligation efficiency, and mild reaction conditions.[11−14] Most reported Cu^{2+} sensors, however, without signal amplification strategies, suffer from relatively low detection sensitivity. To overcome this drawback, several reports of adopting multi-invertase conjugated magnetic bead signal amplification strategy[15] or catalytic hairpin assembly (CHA)[16] achieved sensitive detection of Cu^{2+}. Although the above studies improved the sensitivity of Cu^{2+} monitoring to some extent, the detecting sensitivity is still limited due to the lack of highly efficient amplification strategy, which cannot satisfy the requirement of trace detection of Cu^{2+} in environmental and biological samples. Hence, it is desirable to explore a highly efficient amplification strategy for the ultrasensitive detection of Cu^{2+}, which represents an advance over traditional analytical methods.

The DNA walking machine, an example of an intelligent and automatically ongoing DNA-based nanomachine, has been considered as an extremely attractive nucleic acid amplification

Received: June 6, 2018
Accepted: September 3, 2018
Published: September 3, 2018

DOI: 10.1021/acs.analchem.8b02555
Anal. Chem. 2018, 90, 11439−11445

Scheme 1. (A) Fabrication Process of Click Chemistry Reaction-Activated 3D DNA Walking Machine. (B) Electrode Modification and Signal Output Process on the Electrode with Catalytic Hairpin Assembly (CHA)

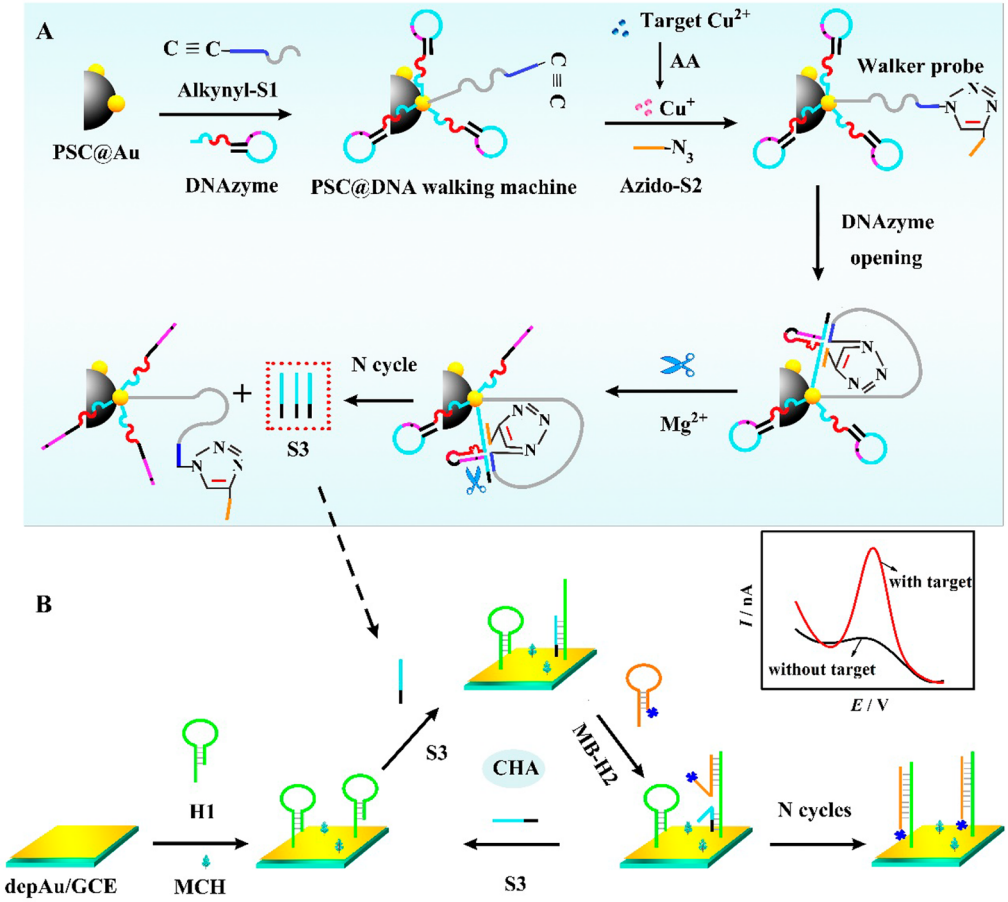

tool due to its inherent advantages of high cargo loading capacity, accelerated target-recycling kinetics, and protein motor imitation.[17,18] Powered by energy-containing hybridization,[19] hydrolysis,[20] and conformational change[21,22] of DNA, the DNA walking machine can walk progressively along the tracks to achieve cargo transit and target detection. However, most DNA walking machines have been built on one-dimensional or two-dimensional tracks,[23−25] which have the common limitation of low mobility and cargo payload. Impressively, the three-dimensional (3D) DNA walking machine, performing on 3D nanomaterials, possesses increased walking steps and satisfactory signal amplification of nucleic acids[26] or protein detection,[27] because of the improved mobility of the walker and high DNA loading efficiency.[28,29] In this contribution, a 3D DNA walking machine triggered by click chemistry ligation between azido-modified DNA and alkynyl-modified DNA is proposed for ultrasensitive electrochemical detection of Cu^{2+}.

In this work, we have for the first time applied click chemistry reaction to a 3D DNA walking machine for developing a sensitive electrochemical biosensor for Cu^{2+} detection, which couples the high selectivity of click chemistry reaction with dual-amplification strategy of the 3D DNA walking machine and catalytic hairpin assembly (CHA) recycling. As shown in Scheme 1A, the prepared machine was composed of azido-labeled S2 (azido-S2), alkynyl-labeled S1 (alkynyl-S1), and hairpin-locked DNAzyme[30] track-assembled on aminated magnetic polystyrene microsphere@gold nanoparticles (PSC@Au) by the Au−S bond. In the absence of target Cu^{2+}, the alkynyl- and azido-DNA were unable to bind for the hairpin-locked DNAzyme strand opening. Upon the addition of target Cu^{2+}, Cu^{+} was in-site generated through the reduction of Cu^{2+} with help from sodium ascorbate (AA), which specifically and efficiently triggered the click chemistry between azido on S2 and alkynyl on S1, resulting in the formation of a walker probe on PSC@Au. Then the walker probe caused an unfolding of hairpin-structured DNAzyme. In the presence of cofactor magnesium ion (Mg^{2+}), the unlocked DNAzyme was activated to cleave the self-strand at the ribonucleotide site, accompanied by the release of product DNA (S3) and walker probe from the DNAzyme strand. Therefore, the walker probe was able to open the adjacent hairpin-locked DNAzyme strand and then be released by DNAzyme cleavage along the PSC@Au-DNAzyme track. With the amplification strategy of the 3D DNA walking machine, a large number of S3 were produced to trigger CHA recycling. Simultaneously, as displayed in Scheme 1B, thiol-labeled hairpin DNA (H1) was covalently attached to a gold nanoparticle-assembled glassy carbon electrode (depAu/GCE) via the Au−S bond. Next, mercaptohexanol (MCH) was employed to backfill the unspecific sites of the electrode. When the obtained single-strand S3 was introduced onto the sensor, S3 could combine with H1 to open the hairpin structure of H1, generating a DNA duplex with an exposed tail. In this case, the exposed tail of H1 hybridized with the methylene blue-tagged hairpin DNA (MB-H2),

DOI: 10.1021/acs.analchem.8b02555
Anal. Chem. 2018, 90, 11439−11445

triggering CHA recycling and releasing S3. The liberated S3 could thus bind with another H1, and the reaction was switched again, achieving the attachment of plenty of MB-H2 onto the electrode with notable electrochemical responses. As a result, the coupling of click chemistry reaction with the 3D DNA walking machine enabled the proposed biosensor to detect Cu^{2+} with high selectivity. With the dual-amplification strategy of the 3D DNA walking machine and CHA recycling, this biosensor exhibited high sensitivity for tracing Cu^{2+} in real samples. Moreover, the elaborated biosensor could be employed for determination of Mg^{2+}, which paved the way to applications of the 3D DNA walking machine in the sensing of various ions.

EXPERIMENTAL SECTION

Chemicals and Materials. Aminated magnetic polystyrene microspheres (NH_2-PSC) were supplied by Tianjin BaseLine ChromTech Research Centre (Tianjin, China). Hydrogen tetrachloroaurate ($HAuCl_4 \cdot 4H_2O$, 99.9%), mercaptohexanol (MCH), and sodium ascorbate (AA) were purchased from Sigma Chemical Co. (St. Louis, MO). Tris(2-carboxyethyl)phosphine hydrochloride (TCEP) and DNA oligonucleotides were provided by Sangon Biotech Co., Ltd. (Shanghai, China). The corresponding sequences are listed in Table S1.

Apparatus. Electrochemical impedance spectroscopy (EIS), cyclic voltammetry (CV), and square wave voltammetry (SWV) were performed on a CHI 660D electrochemistry workstation (Shanghai Chenhua Instrument Co., Ltd., China) with a conventional three-electrode system.[31] Polyacrylamide gel electrophoresis (PAGE) was recorded on a Bio-Rad imaging system (Hercules, CA).

Preparation of a 3D DNA Walking Machine Modified on PSC. Modification of aminated PSC with a 3D DNA walking machine was synthesized by Au−N coupling. First, 500 μL of NH_2-PSC (5 mg mL^{-1}) was washed with ultrapure water sufficiently, whereafter 5 mL of 20 nm citrate-stabilized AuNP solution was added.[32] After 1 h of incubation at 4 °C, the obtained PSC@Au nanocomposites were washed three times and resuspended into 1 mL of phosphate buffer (PBS, 0.1 M, pH 7.4). Meanwhile, DNAzyme was heated to 95 °C for 5 min and slowly cooled to room temperature. For preventing disulfide formation, all thiol-modified oligonucleotides were preincubated with 10 mM TCEP solution for 40 min. Afterward, a mixture of 200 μL of PSC@Au, 200 μL of DNAzyme (5 μM), and 10 μL of S1 (5 μM) was incubated at room temperature for 12 h. To maximize the loading amounts of oligonucleotides,[33] 17 μL of NaCl solution (1 M) was added into the above solution mixture and repeated five times at a 1 h interval. After incubation at room temperature for another 24 h, the solution was magnetically separated to remove unconjugated oligonucleotides. Finally, the PSC@Au-DNA assembly was washed three times and then stored in 200 μL of PBS (0.1 M, pH 7.4) for the following experiment.

Fabrication of the Electrochemical Biosensor. First, a glassy carbon electrode (GCE) was pretreated with alumina slurry (0.3 and 0.05 μm) and then coated with a layer of AuNPs (depAu) by electrodepositing in 2 mL of $HAuCl_4$ solution (1%) at −0.2 V for 30 s. Then 10 μL of thiol-H1 (2.0 μM) was dropped onto the above electrode (depAu/GCE) and incubated at room temperature overnight. Finally, the nonspecific binding sites of modified electrode were blocked with 10 μL of MCH (1.0 mM) for 40 min.

Operation of Click Chemistry Reaction-Triggered 3D DNA Walking Machine. The ligation of alkynyl-S1 with azido-S2 was performed by mixing 8 μL of azido-S2 (5 μM), 1 μL of Cu^{2+} (various concentration), 1 μL of AA (2-fold relative to the concentration of Cu^{2+}), and 90 μL of the prepared PSC@Au-alkynyl-S1, followed by incubating at room temperature for 90 min. Afterward, the mixture was separated with a magnet to remove unconjugated azido-S2 and resuspended into 90 μL of PBS buffer (0.1 M, pH 7.4). Then 10 μL of Mg^{2+} solution (10 μM) was added into the above solution and incubated at 37 °C for 4 h. Finally, the product DNA (S3) solution was separated with a magnet for to further induce catalyzed hairpin assembly (CHA) on the electrode surface.

Experimental Measurements. Before electrochemical measurement, the modified electrode was immersed in a mixture containing 10 μL of methylene blue-labeled H2 (MB-H2, 2 μM) and 10 μL of the obtained S3 at 37 °C for 2 h to conduct CHA recycling. Afterward, the electrochemical biosensor was immersed in 2 mL of PBS buffer (0.1 M, pH 7.4) for SWV detection from −0.6 to 0 V at a frequency of 25 Hz.

Gel Electrophoresis. A 16% freshly prepared polyacrylamide gel was prepared with 5× TBE buffer (445 mM Tris, 445 mM boric acid, 10 mM EDTA, pH 8.0). Electrophoresis was run at 120 V for 2.5 h in 1× TBE buffer. After being stained by ethidium bromide (EB), the gel was viewed under UV light. Detailed reaction conditions for the samples are the same as in the electrochemical assay.

RESULTS AND DISCUSSION

Polyacrylamide Gel Electrophoresis (PAGE) Characterization. The feasibility of click chemistry reaction-triggered 3D DNA walking machine operation and CHA reaction was characterized by PAGE (16%). As shown in Figure 1, the single bands in lanes 1, 2, 5, 8, and 9 represented the individual nucleotides of S1 (4 μM), S2 (4 μM), hairpin-locked

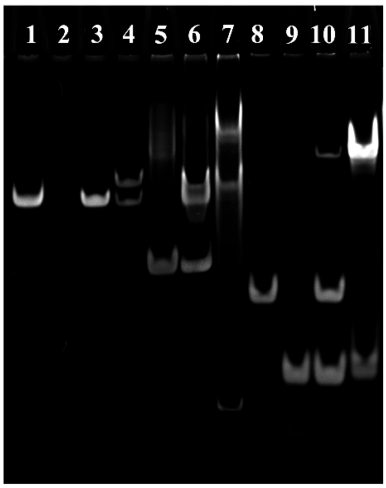

Figure 1. PAGE analysis for different samples: lane 1, single-stranded DNA S1; lane 2, single-stranded DNA S2; lane 3, the mixture of S1 and S2 without target; lane 4, the mixture of S1 and S2 with target and AA; lane 5, hairpin-locked DNAzyme strand; lane 6, the mixture of hairpin-locked DNAzyme strand, S1, and S2; lane 7, amplification products of the click chemistry reaction-triggered 3D DNA walking machine; lane 8, hairpin H1; lane 9, hairpin H2; lane 10, annealing of H1 and H2; lane 11, the mixture of products S3, H1, and H2.

DOI: 10.1021/acs.analchem.8b02555
Anal. Chem. 2018, 90, 11439−11445

DNAzyme strand (2 μM), H1 (0.5 μM), and H2 (0.5 μM), respectively. Compared with the mixture of S1 and S2 (lane 3), the mixture of S1, S2, Cu^{2+} (10 μM), and AA (20 μM) generated a clear band with a higher molecular weight (lane 4), which indicated the ligation of S2 and S1. S1 and S2 did not hybridize with DNAzyme (lane 6 vs 1, 2, and 5) because the walker probe did not form. When cofactor Mg^{2+} (1 μM) was added into the mixture of DNAzyme, S1, S2, Cu^{2+}, and AA, a bright band with increased molecular weight and a blurry band with the fastest mobility were observed (lane 7), owing to the hybridization of the walker probe with DNAzyme and the self-cleavage of DNAzyme. As a control test, the annealing reaction of H1 with H2 in the absence of products S3 was investigated by PAGE. As shown in lane 10, two bright bands corresponding to H1 and H2 and an indistinct band of the H1/H2 duplex could be obviously observed. After introduction of products S3, the hybridization of the H1/H2 duplex (lane 11) was facilitated in contrast to hybridization by the annealing of hairpin H1 and H2 (lane 10). These results demonstrated that the progression of the click chemistry reaction-triggered 3D DNA walking machine could generate S3 to further trigger the CHA reaction on the electrode.

Electrochemical Characterization of the Modified Electrode. To investigate the stepwise fabrication process for the modified electrode, CV and EIS were performed in PBS (0.1 M, containing 5 mM $[Fe(CN)_6]^{3-/4-}$). As shown in Figure 2A, relative to the bare GCE (curve a), modification of

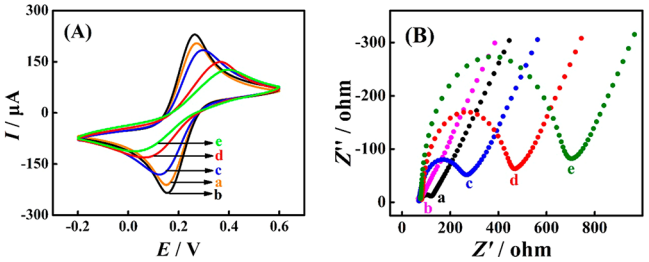

Figure 2. (A) CV and (B) EIS characterization of modified electrode in 5 mM $[Fe(CN)_6]^{3-/4-}$ electrolyte: (a) bare GCE, (b) depAu/GCE, (c) thiol-H1/depAu/GCE, (d) MCH/thiol-H1/depAu/GCE, and (e) MB-H2/MCH/thiol-H1/depAu/GCE.

the AuNPs caused an increasing redox peak current (curve b) because they could promote electron transfer between $[Fe(CN)_6]^{3-/4-}$ and the electrode. When thiol-H1 was modified on the sensing interface, however, the redox peak decreased (curve c), owing to electrostatic repulsion between $[Fe(CN)_6]^{3-/4-}$ and the negatively charged phosphate backbones of thiol-H1.[34,35] Moreover, the redox peak decreased again (curve d) upon introduction of nonconductive MCH to block the nonspecific site of the sensing interface. Undoubtedly, a further decreased redox peak was observed after incubating a mixture of MB-H2 and product S3 (curve e), owing to the fact that more negatively charged phosphate backbones were introduced onto the electrode surface.

Figure 2B showed impedance curves of the stepwise modification process. Compared with the bare GCE (curve a), the value of electron-transfer resistance (R_{et}) of depAu/GCE decreased (curve b) owing to the conductivity of the AuNPs. After negatively charged thiol-H1 (curve c) and nonconductive MCH (curve d) were sequentially modified onto the electrode, however, the value of R_{et} increased continually. When the electrode was incubated with a mixture of MB-H2 and S3, the value of R_{et} increased greatly (curve e). These results indicated the successful fabrication of the modified electrode according to Scheme 1.

Optimization of the Experimental Conditions. Because the amplification efficiency of the 3D DNA walking machine relies on both the click chemistry reaction and the Mg^{2+}-dependent DNAzyme cleavage, the concentration ratio between S1 and DNAzyme was optimized in this study. To investigate the optimal ratio, the proposed biosensor was evaluated by using SWV with six ratios (from 1:5 to 1:30). With the increase of ratio from 1:5 to 1:20, the current response increased and reached a plateau after 1:20. Therefore, 1:20 was chosen as the optimal ratio for subsequent experiments (Figure 3A).

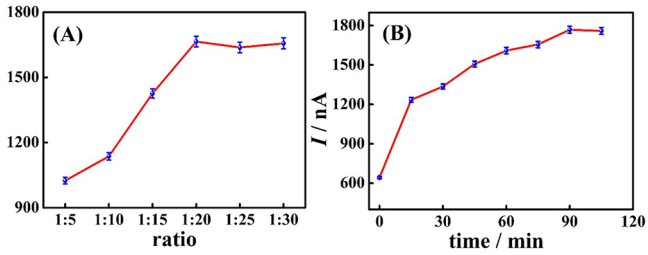

Figure 3. (A) Influence of the concentration ratios between S1 and DNAzyme toward SWV response (ratios between S1 and DNAzyme: 1:5, 1:10, 1:15, 1:20, 1:25, 1:30. (B) Effect of click chemistry reaction time toward SWV response (time: 0, 15, 30, 45, 60, 75, 90, 105 min).

Under the above optimal condition, the click chemistry reaction time was also optimized at room temperature. The proposed biosensor was studied by SWV in the presence of Cu^{2+} (100 nM) at a time interval of 15 min (0, 15, 30, 45, 60, 75, 90, 105 min). As shown in Figure 3B, the SWV response increased rapidly with prolonged reaction time and tended to level off after 90 min. Therefore, 90 min was enough for click chemistry. We also used polyacrylamide gel electrophoresis to examine the click chemistry time, and similar results were obtained (Figure S1).

Effect of Cu^{2+} and Mg^{2+} on the Analytical Performance of the Biosensor. The target Cu^{2+} and cofacter Mg^{2+} were important elements for click chemistry reaction-triggered 3D DNA walking machine operation, which affects the analytical performance of the biosensor. Therefore, the proposed biosensor was investigated by SWV in the presence/absence of target Cu^{2+} with/without Mg^{2+} (Figure 4). When the biosensor was incubated with 0 nM Cu^{2+}, the

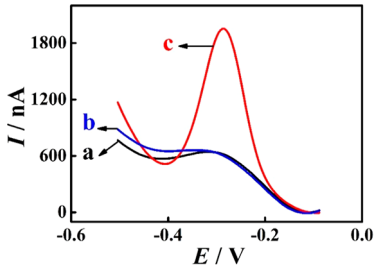

Figure 4. SWV response of the biosensor incubated with 0 nM Cu^{2+} (curve a), 500 nM Cu^{2+} without Mg^{2+} (curve b), and 500 nM Cu^{2+} with 1 μM Mg^{2+} (curve c).

DOI: 10.1021/acs.analchem.8b02555
Anal. Chem. 2018, 90, 11439−11445

alkynyl- and azido-DNA were unable to bind to the hairpin-locked DNAzyme strand opening and none of the product S3 was released, which was consistent with the result that a low SWV response was observed (curve a). In the presence of 500 nM Cu^{2+} but without Mg^{2+}, the SWV response barely changed (curve b), suggesting that the DNAzyme was not activated to cleave the self-strand for generating product S3. When 500 nM Cu^{2+} and 1 μM Mg^{2+} were modified on the sensing surface, the SWV current increased dramatically (curve c). This might be ascribed to the fact that amounts of single-strand S3 were generated by the 3D DNA walking machine, resulting in the capture of many MB-DNAs onto the sensor surface with dramatically increased SWV response. Therefore, this biosensor not only can realize detection of Cu^{2+} but can also be employed for Mg^{2+} detection.

Analytical Performance of the Biosensor toward Cu^{2+}. To investigate the analytical performance of the click chemistry reaction-triggered 3D DNA walking machine, the proposed biosensor was incubated with Cu^{2+} standard solution with different concentrations and analyzed by SWV. As shown in Figure 5A, the SWV response increased with incremental

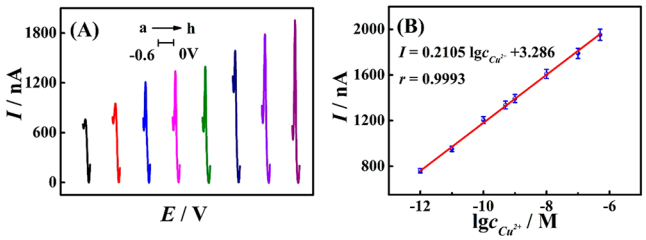

Figure 5. (A) SWV response of the biosensor with various concentrations of Cu^{2+} (1 pM, 10 pM, 100 pM, 500 pM, 1 nM, 10 nM, 100 nM, 500 nM) in 0.1 M PBS (pH 7.4). (B) Calibration plot of SWV response vs the logarithm of Cu^{2+} concentration.

Cu^{2+} concentration. Figure 5B showed that the SWV response was proportional to the Cu^{2+} concentration from 1.0 pM to 500 nM with a regression equation expressed as I = 0.2105 lg $c_{Cu}{}^{2+}$ + 3.286, and the correlation coefficient was 0.9993. A detection limit of 0.33 pM for the target could be estimated. As shown in Table 1, the proposed click chemistry reaction-triggered 3D DNA walking machine strategy showed enhanced sensitivity and wider linear range compared with other reported methods, which should be attributed to the integration of the high selectivity of the click chemistry reaction with the dual-amplification strategy of the 3D DNA walking machine and CHA recycling. Nevertheless, this developed sensing platform consisted of 3D DNA walking machine operation and electrode assembly, which was often subject to complicated operation. Therefore, future development to construct a rapid, simple, and convenient sensing platform is urgently needed.

Table 1. Comparison of Different Methods for Cu^{2+} Analysis

methods	strategies	linear range	detection limit	refs
colorimetric	click chemistry	50 nM to 50 μM	5.9 nM	14
fluorescent	CdSe/ZnS QDs	30 nM to 600 nM	0.15 nM	36
fluorescent	Cu^{2+}-dependent DNAzyme	10 pM to 200 nM	1.0 pM	37
electrochemical	Cu^{2+}-glycine	0.5 nM to 30 nM	42.4 pM	38
electrochemical	TPAASH	0.6 μM to 11 μM	80.3 nM	39
electrochemical	metal−organic frameworks	5.0 pM to 900 nM	1.0 pM	6
electrochemical	click chemistry	1.0 pM to 500 nM	0.33 pM	this work

Specificity, Reproducibility, and Stability of the Proposed Biosensor. To further evaluate the specificity, Ag^{+}, Ca^{2+}, Mg^{2+}, Cd^{2+}, Hg^{2+}, Pb^{2+}, Co^{2+}, Mn^{2+}, Fe^{2+}, and Cr^{3+} (10 μM, respectively) were chosen as interfering ions, whose concentration was 100-fold relative to the concentration of Cu^{2+} (100 nM). As shown in Figure 6, compared with the

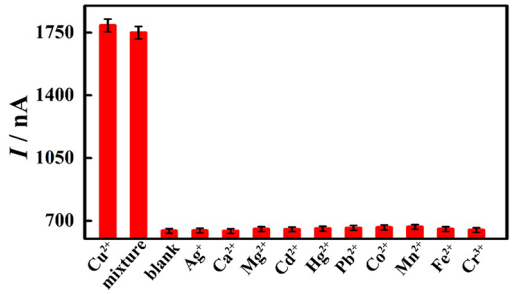

Figure 6. Specificity of the electrochemical biosensor toward mixture control, blank control, and different interferences: Ag^{+}, Ca^{2+}, Mg^{2+}, Cd^{2+}, Hg^{2+}, Pb^{2+}, Co^{2+}, Mn^{2+}, Fe^{2+}, and Cr^{3+}. The concentration of each interfering ion was 10 μM, which was 100-fold more than that of target Cu^{2+} (100 nM).

blank control, no significant SWV responses from interfering ions were observed except that of target Cu^{2+} (100 nM). In addition, while 100 nM Cu^{2+} coexisted with all interfering ions (10 μM, respectively), the SWV response of the mixture was almost unchanged in comparison with the case of only target Cu^{2+}. These results indicated good specificity of this strategy for Cu^{2+} detection. The reproducibility of the biosensor was studied by interassay (the same electrode toward 100 nM Cu^{2+} was detected five times) and intra-assay (five electrodes were used with 100 nM Cu^{2+}). The relative standard deviation (RSD) of interassay and intra-assay was 4.2% and 6.1%, respectively, demonstrating that the reproducibility was acceptable. The stability was monitored by storing the biosensor at 4 °C and assaying every 3 days by SWV. After 15 days, the SWV response retained 90.6% of its initial current, suggesting that the biosensor had acceptable stability.

Recovery Test. To investigate the application potential of the developed biosensor, a recovery experiment was adopted. Briefly, tap water samples, obtained from the tap in our laboratory, were used to prepare various concentrations of Cu^{2+}. From Table 2, we could see that the recovery ranged from 98.8% to 105% and RSDs varied from 2.2% to 9.4%, suggesting that our proposed strategy was promising for Cu^{2+} detection in tap water.

CONCLUSION

In this work we developed a highly selective and ultrasensitive approach for electrochemical detection of Cu^{2+} by coupling the click chemistry reaction-triggered 3D DNA walking machine with CHA recycling, which demonstrated attractive features relative to traditional detection of Cu^{2+}. Click chemistry

DOI: 10.1021/acs.analchem.8b02555
Anal. Chem. 2018, 90, 11439−11445

Table 2. Recovery Results of the Proposed Biosensor in Tap Water

samples	added (nM)	found (nM)[a]	recovery (%)	RSD (%)
1	0.100	0.102	102	5.6
2	0.500	0.506	101	2.2
3	1.00	1.05	105	9.4
4	10.0	10.1	101	3.5
5	100	98.8	98.8	4.4

[a]Mean value of four parallel determinations in the optimal experiment conditions.

reaction was applied for the first time to initiate the 3D DNA walking machine, which enabled the proposed biosensor with high selectivity toward Cu^{2+} detection. Based on the dual-amplification strategy of the 3D DNA walking machine and CHA recycling, the sensitivity of the designed biosensor was greatly enhanced. Interestingly, it can be readily extended for the detection of Mg^{2+}, offering great potential for the detection of various ions in diverse fields such as clinical diagnosis and environmental areas.

■ ASSOCIATED CONTENT

Supporting Information

The Supporting Information is available free of charge on the ACS Publications website at DOI: 10.1021/acs.analchem.8b02555.

The oligonucleotide sequences used in this work, investigation of click chemistry reaction time by PAGE, estimation of the surface coverage of DNAzyme on the PSC@AuNPs, and calculation of the surface coverage of H1 on the depAu/GCE (PDF)

■ AUTHOR INFORMATION

Corresponding Authors

*Tel: +86-23-68252277. Fax: +86-23-68253172. E-mail: yuanruo@swu.edu.cn.

*Tel: +86 23 49891969. Fax: +86 23 61162725. E-mail: tangying@cqwu.edu.cn.

ORCID

Dianyong Tang: 0000-0001-9389-870X

Ruo Yuan: 0000-0003-3664-6236

Notes

The authors declare no competing financial interest.

■ ACKNOWLEDGMENTS

This work was financially supported by the NNSF of China (21705013, 21775124), the Chongqing Science and Technology Commission of China (cstc2017jcyjAX0282, cstc2015jcyjBX0126, cstc2016shmsZX20001), the Science and Technology Research Program of Chongqing Municipal Education Commission China (KJ1711265), Chongqing University of Arts and Sciences, China (M2017 ME11), and Chongqing Key Laboratory of Environmental Materials and Remediation Technology (Chongqing University of Arts and Sciences) (CEK1703).

■ REFERENCES

(1) Boal, A. K.; Rosenzweig, A. C. *Chem. Rev.* **2009**, *109*, 4760−4779.

(2) Cotruvo, J. A., Jr.; Aron, A. T.; Ramos-Torres, M. K.; Chang, C. *Chem. Soc. Rev.* **2015**, *44*, 4400−4414.

(3) Jo, J.; Lee, H. Y.; Liu, W. J.; Olasz, A.; Chen, C. H.; Lee, D. *J. Am. Chem. Soc.* **2012**, *134*, 16000−16007.

(4) Zhao, X. P.; Wang, S. S.; Younis, M. R.; Xia, X. H.; Wang, C. *Anal. Chem.* **2018**, *90*, 896−902.

(5) Li, L.; Feng, J.; Fan, Y. Y.; Tang, B. *Anal. Chem.* **2015**, *87*, 4829−4835.

(6) Jin, J. C.; Wu, J.; Yang, G. P.; Wu, Y. L.; Wang, Y. Y. *Chem. Commun.* **2016**, *52*, 8475.

(7) Li, Z. P.; Zhang, Y. W.; Xia, H.; Mu, Y.; Liu, X. M. *Chem. Commun.* **2016**, *52*, 6613.

(8) Wu, R.; Zhang, S. H.; Lyu, J. T.; Lu, F.; Yue, X. F.; Lv, J. G. *Chem. Commun.* **2015**, *51*, 8078.

(9) Zhao, Z.; Chen, H. D.; Zhang, H.; Ma, L. N.; Wang, Z. X. *Biosens. Bioelectron.* **2017**, *91*, 306−312.

(10) Wang, F.; Orbach, R.; Willner, I. *Chem. - Eur. J.* **2012**, *18*, 16030−16036.

(11) Shen, Q. P.; Tang, S. Y.; Li, W. H.; Nie, Z.; Liu, Z. L.; Huang, Y.; Yao, S. Z. *Chem. Commun.* **2012**, *48*, 281−283.

(12) Zhou, Y.; Wang, S. X.; Zhang, K.; Jiang, X. Y. *Angew. Chem.* **2008**, *120*, 7564−7566.

(13) Lei, Y. M.; Xiao, B. Q.; Liang, W. B.; Chai, Y. Q.; Yuan, R.; Zhuo, Y. *Biosens. Bioelectron.* **2018**, *109*, 109−115.

(14) Ge, C. C.; Luo, Q.; Wang, D.; Zhao, S. M.; Liang, X. L.; Yu, L. X.; Xing, X. R.; Zeng, L. W. *Anal. Chem.* **2014**, *86*, 6387−6392.

(15) Su, J.; Xu, J.; Chen, Y.; Xiang, Y.; Yuan, R.; Chai, Y. Q. *Biosens. Bioelectron.* **2013**, *45*, 219−222.

(16) Li, D. X.; Zhou, W. J.; Chai, Y. Q.; Yuan, R.; Xiang, Y. *Chem. Commun.* **2015**, *51*, 12637.

(17) Zhou, C.; Duan, X. Y.; Liu, N. *Nat. Commun.* **2015**, *6*, 8102.

(18) Zhang, P.; Jiang, J.; Yuan, R.; Zhuo, Y.; Chai, Y. Q. *J. Am. Chem. Soc.* **2018**, *140*, 9361−9364.

(19) Yeo, Q. Y.; Loh, I. Y.; Tee, S. R.; Chiang, Y. H.; Cheng, J.; Liu, M. H.; Wang, Z. S. *Nanoscale* **2017**, *9*, 12142.

(20) Qu, X. M.; Zhu, D.; Yao, G. B.; Su, S.; Chao, J.; Liu, H. J.; Zuo, X. L.; Wang, L. H.; Shi, J. Y.; Wang, L. H.; Huang, W.; Pei, H.; Fan, C. H. *Angew. Chem.* **2017**, *129*, 1881−1884.

(21) You, M. X.; Chen, Y.; Zhang, X. B.; Liu, H. P.; Wang, R. W.; Wang, K. L.; Williams, K. R.; Tan, W. H. *Angew. Chem., Int. Ed.* **2012**, *51*, 2457−2460.

(22) Ma, P. Q.; Liang, C. P.; Zhang, H. H.; Yin, B. C.; Ye, B. C. *Chem. Sci.* **2018**, *9*, 3299−3304.

(23) Liu, X. Q.; Niazov-Elkan, A.; Wang, F.; Willner, I. *Nano Lett.* **2013**, *13*, 219−225.

(24) Cha, T. G.; Pan, J.; Chen, H. R.; Robinson, H. N.; Li, X.; Mao, C. D.; Choi, J. H. *J. Am. Chem. Soc.* **2015**, *137*, 9429−9437.

(25) Liber, M.; Tomov, T. E.; Tsukanov, R.; Berger, Y.; Nir, E. *Small* **2015**, *11*, 568−575.

(26) Yang, X. L.; Tang, Y. N.; Mason, S. D.; Chen, J. B.; Li, F. *ACS Nano* **2016**, *10*, 2324−2330.

(27) Chen, J. B.; Zuehlke, A.; Deng, B.; Peng, H. Y.; Hou, X. D.; Zhang, H. Q. *Anal. Chem.* **2017**, *89*, 12888−12895.

(28) Jiang, X. Y.; Wang, H. J.; Wang, H. J.; Zhuo, Y.; Yuan, R.; Chai, Y. Q. *Anal. Chem.* **2017**, *89*, 4280−4286.

(29) Peng, H. Y.; Li, X. F.; Zhang, H. Q.; Le, X. C. *Nat. Commun.* **2017**, *8*, 14378.

(30) Yang, Y. J.; Huang, J.; Yang, X. H.; He, X. X.; Quan, K.; Xie, N. L.; Ou, M.; Wang, K. M. *Anal. Chem.* **2017**, *89*, 5851−5857.

(31) Cheng, F. F.; He, T. T.; Miao, H. T.; Shi, J. J.; Jiang, L. P.; Zhu, J. J. *ACS Appl. Mater. Interfaces* **2015**, *7*, 2979−2985.

(32) Vetten, M. A.; Tlotleng, N.; Rascher, D. T.; Skepu, A.; Keter, F. K.; Boodhia, K.; Koekemoer, L. A.; Andraos, C.; Tshikhudo, R.; Gulumian, M. *Part. Fibre Toxicol.* **2013**, *10*, 50.

(33) Hurst, S. J.; Lytton-Jean, A. K. R.; Mirkin, C. A. *Anal. Chem.* **2006**, *78*, 8313−8318.

(34) Wu, L.; Ding, F.; Yin, W. M.; Ma, J.; Wang, B. R.; Nie, A. X.; Han, H. Y. *Anal. Chem.* **2017**, *89*, 7578.

(35) Yang, J. M.; Dou, B. T.; Yuan, R.; Xiang, Y. *Anal. Chem.* **2017**, *89*, 5138−5143.

(36) Jin, L. H.; Han, C. S. *Anal. Chem.* **2014**, *86*, 7209−7213.

DOI: 10.1021/acs.analchem.8b02555
Anal. Chem. 2018, 90, 11439−11445

(37) Xiong, Y. M.; Meng, P. J.; Li, H. L.; Hu, Y.; Zhou, L. H.; Jiang, S. Q.; Pang, Y. F.; Li, S. J.; Huang, P. L. *Chem. Commun.* **2018**, *54*, 2542−2545.
(38) Li, J. P.; Zhang, L. M.; Wei, G.; Zhang, Y.; Zeng, Y. *Biosens. Bioelectron.* **2015**, *69*, 316−320.
(39) Zhang, L. M.; Han, Y. Y.; Zhao, F.; Shi, G. Y.; Tian, Y. *Anal. Chem.* **2015**, *87*, 2931−2936.

DOI: 10.1021/acs.analchem.8b02555
Anal. Chem. 2018, 90, 11439−11445